Egyptian Journal of Chemistry

http://ejchem.journals.ekb.eg/

3D-QSAR, ADMET, and Molecular Docking Studies for Designing New 1,3,5-Triazine Derivatives as Anticancer Agents

Reda El-Mernissi, [1,*] Khalil El Khatabi,[1] Ayoub Khaldan,[1] Larbi El Mchichi,[1] Mohammed Aziz Ajana,[1,*] Tahar Lakhlifi,[1] Mohammed Bouachrine[1,2]

[1]University of Moulay Ismail, Faculty of Science, MCNSL, Meknes, Morocco.
[2]EST Khenifra, Sultan Moulay Sliman University, Benimellal, Morocco.

Abstract

Cancer is one of the world's causes of death, which requires the discovery of new molecules likely to become anticancer drugs. In this study, three – dimensional Quantitative Structure-Activity Relationship is employed to study thirty compounds of 1,3,5-triazine derivatives against cancer cell lines (human lung adenocarcinoma cells A549). Their pIC$_{50}$ varied from 4.29 to 6.70. In addition, the 3D-QSAR model was defined based on Comparative Molecular Field Analysis (CoMFA) and Comparative Molecular Similarity Indices (CoMSIA) analysis. The model CoMFA and CoMSIA indicate strong reliability with ($Q^2 = 0.70$; $R^2 = 0.92$; $r_{test}^2 = 0.96$) and ($Q^2 = 0.62$; $R^2 = 0.86$; $r_{test}^2 = 0.98$), respectively. We have proposed four compounds with highly potent anticancer predicted activities, based on successful results obtained by the contour maps formed by the method model. Furthermore, the ADMET properties of these newly designed compounds were in silico evaluated, among which three derivatives have respected these properties. These compounds were further evaluated by molecular docking, showing that two molecules **X$_2$** and **X$_4$** exhibit favorable interactions with the targeted receptor and a high total score. These findings may provide valuable information for further need to discover potent PI3Ks inhibitors.

Keywords: Cancer, 1,3,5- triazine, 3D- QSAR, ADMET, Molecular docking ;

1. Introduction

Cancer is one of the most widespread diseases in the world, where there are over 100 different types of cancer. This disease can affect any organ in the human body. The most frequently encountered cancers in the world are lung, breast, and prostate cancers. The 3-kinases phosphatidylinositol (PI3Ks) are grouped into three groups (I – III), that vary in function and structure. Enzymes in class were intensively studied and emerged as promising targets for drugs in immune disorders and cancer. The class I, PI3K, has a long history of cancer association, phosphatidylinositol 3-kinase (PI3K)/protein kinase B (AKT)/mammalian signaling pathway for rapamycin (mTOR) plays a significant role in a variety of cellular functions, like proliferation, cell development, motility, survival, and differentiation. The PI3K/AKT/mTOR pathway was discovered to be dysregulated in nearly every human cancer, which has been identified as a promising target for cancer therapy (1-5). The phosphoinositide 3-kinase (PI3K) process is a key signal transduction mechanism that connects multiple receptor groups and oncogenes to several important cell activities. Recently, the Food and Drug Administration (FDA) approved some PI3K inhibitor products, such as Idelalisib (GS-1101) (6), Copanlisib (BAY 80-6946) (7), and Alpelisib (BYL719) (8). In recent years, researchers have found that novel PI3K / mTOR dual inhibitors, for example GSK2126458 (9), Apitolisib (G DC-09 80) (10), and PI-103 (11), and defined A549 cells in 1972. These inhibitors are used in the development of drug therapies as research models against cancer (12-13). The PI3K/AKT/mTOR channel pathway is the most altered in cancers. Also, it is often activated via a transmembrane receiver such as RTKs. If these receptors are activated, they will recruit the PI3Ks proteins according to sequence homology and substrate preference. By following activation of an RTK, class IA of PI3K which is recruited to the plasma membrane and binds to the

_____

_____

phospho-tyrosines of the receptor via the SH2 domains (Srchomology) of its p85a subunit (14). The PI3K class I phosphorylate the D3 part of phosphatidylinositol (PtdIns) membranes. PtdIns-4,5-diphosphate (PtdIns [4,5]-P2) is phosphorylated to PtdIns-3,4,5-triphosphate (PtdIns [3,4,5]-P3), providing a binding site at the membrane for serine/threonine kinase protein, Akt. Once activated, it is released in the cytosol or is translocated in the nucleus to phosphorylate substrates involved in the progression of the cell cycle, metabolism, survival, apoptosis, and translation (15). The mammalian target of Rapamycin (mTOR) is the most studied target of Akt. It consists of three main areas, the first FRB domain (FKBP12-rapamycin binding), the catalytic one, and the HEAT domain (huntingtin-elongation-A subunit-TOR) (16). Recent studies have shown that the mTOR protein exists as two different complexes, mTORC1 and mTORC2. The mTORC1 complex is regulated by signaling pathways PI3K/Akt and MAPK. The activation of p70S6K/mTORC1 also serves as negative feedback to reduce the activity of the PI3K pathway through the phosphorylation of insulin receptor substrate 1 and 2 (IRS1 and IRS2), which interrupts the signaling between IGF1R and PI3K (17). The aberrant activation of the PI3K/ AKT /mTOR pathway plays a major role in the mechanisms of resistance to hormone therapy and constitutes a privileged target for the treatment of cancers, both in terms of prevention and reversion of resistance to hormone therapy. The aim of this research is to design new A549 cell cancer inhibitors. We have used 30 compounds of 1,3,5-triazine derivatives against cancer. These compounds are divided into two types, the first group (1-24), the second group (25-30) according to the preparation methods (18). The fight against cancer is progressing in all areas, which have path the way to the three - dimensional quantitative structure-activity relationship (3D - QSAR) to be used to design new effective anticancer compounds, through the methods of comparative molecular field analysis (CoMFA) and comparative molecular similarity indices (CoMSIA). To determine pharmacokinetic properties and toxicity, the ADMET online was used. To discover the binding modes of compounds with the PI3Kα receptor site (PDB code: 4L23), molecular docking was performed by using surflex-docking, and the reliability of the proposed compounds was achieved.

2. Materials and Methods

3D-QSAR modeling was executed on a set of 30 substituted 1,3,5-triazine derivatives taken from the literature (18). The database was divided into two sets. 25 compounds were selected as a training set and the rest were selected as a test set. The training set was used for the construction of the 3D-QSAR (CoMFA and CoMSIA) model. Moreover, the predictive capacity of this model is measured by the test set. Originally, the IC50 value was observed by unit (μM) and transferred into pIC_{50} as (pIC_{50} = Log $1/IC_{50}$). Figure 1 shows the molecular structure of the substances studied, and Table1 shows the different structures for the test and training substances and their biological activities pIC_{50}.
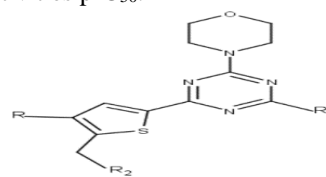

Fig. 1. Structure of the studied compounds.

2.1. Minimization and alignment

Under standard Tripos force field (19), all molecular structures are minimized by using the Gasteiger-Huckel partial atomic charges (20) in the Sybyl (21) program. Molecular alignment (22) is considered as one of the most parameters in 3D-QSAR analyses used to create a performing this model. The database was aligned by using the "align database" command in Sybyl. This procedure requires a molecule template, which is the most active compound 23. The core and alignment of all compounds are shown in figure 2.

2.2. 3D QSAR study

The CoMFA (23) and CoMSIA analysis (24) are used to create 3D QSAR models, to predict new compounds, and to explore various fields, such as steric and electrostatic for the CoMFA model, while CoMSIA gives steric, electrostatic, hydrophobic, H–bond donors and H–bond acceptors. To achieve a linear correlation between the dependent variable (pIC_{50}) and the independent variables (contours), the partial least squares analysis (PLS) (25) regression method was used. The process of non-cross-validation was given to evaluate the coefficient of determination (R^2), the value F (Fischer test and lowest value of standard error of estimates (SEE), while to determine the cross-validated correlation coefficient (Q^2) and the

_____

optimum number of components N, a cross-validation method was used. Furthermore, a test set was used for external validation to calculate r^2ext and estimate the optimal predictive model. The best QSAR model was chosen based on the high Q^2 and the R^2 correlation coefficient should respect the following criterion ($Q^2 > 0.50$ and $R^2 > 0.60$) (25), while r^2ext should have a value of more than 0.6, which in turn indicates the significant predictability of the obtained QSAR model (26).
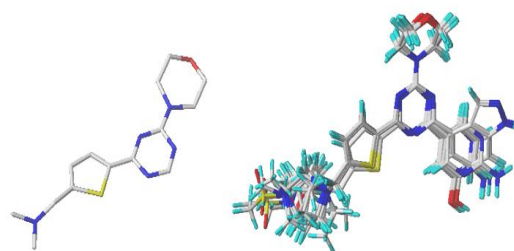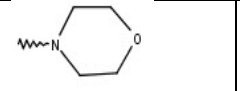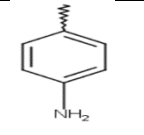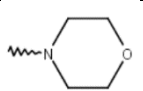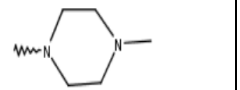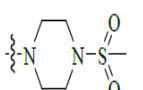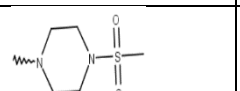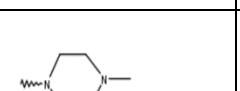

Figure . 2. Core and the alignment of molecules.

Table 1: The structure and activities of studied compounds.

N°	R	R_1	R_2	pIC50	N°	R	R_1	R_2	pIC50
1	H			5.25	17	H			5.32
2	H			5.07	18	H			5.15
3	H			5.33	19*	H			5.94
4	H			4.66	20	H			4.82
5	H			5.63	21*	H			5.82
6	H			5.07	22	H			5.11
7	H			5.95	23	H			6.70
8*	H			4.29	24	H			4.74
9	H			4.88	25	CH3			5 .00
10*	H			4.80	26	CH3			5.18
11	H			5.05	27	CH3			4.93
12	H			4.63	28	CH3			5.37

13	H		(morpholine structure)	5.84	29	CH3	(aminophenyl structure)	(morpholine structure)	5.27
14	H		(N-methylpiperazine structure)	4.67	30*	CH3		(piperazine sulfonyl structure)	5.41
15	H		(piperazine sulfonyl methyl structure)	6.49					
16	H		(N,N-dimethyl piperazine structure)	4.67					

2.3. Y-randomization

The Y-Randomisation was done to affirm the reliability of models obtained (27), where the independent variables of the studied molecules (pIC_{50}) are shuffled several times randomly and a new QSAR model is constructed after every iteration. It is possible to observe the randomized QSAR models with low Q^2 and R^2 values compared to the original models, due to structural redundancy and chance correlation, which indicate a strong and reliable 3D-QSAR model.

2.4. ADMET Prediction

Pharmacokinetics include absorption of the molecule, distribution in the body, elimination including biotransformation or Metabolism, Excretion, and toxic (ADMET). This study used swissadmet web server (28) for predicting the ADMET properties. ADMET prediction is an essential part of the discovery process, where the precise results help to identify the best drug candidates.

2.5. Molecular Docking

To confirm the 3D-QSAR, we have analyzed the binding interactions between the PI3Kα protein (PDB code: 4L23) and ligands. The surflex– Dock (26) module of Sybyl was used for molecular docking studies. The protein and ligands preparation steps for the docking protocol were performed in Discovery Studio 2016 (29). Consequently, the results were observed by using pymol (30).

2.6. Macromolecule preparation

The PI3Kα protein structure (PDB code: 4L23) obtained from the Protein Databank PDB site (www.rcsb.org) was prepared by using Discovery Studio 2016.

2.7. Ligand preparation

By using the SKETCH option in Sybyl software, the 3D structure of the highest active compound (23) and the proposed compounds were formed. Three-dimensional structures were minimized under the Tripos standard force field with Gasteiger-Hückel atomic partial charges by conjugate gradient method with a gradient convergence criterion of 0.01 kcal/mol Å.

3. Results and discussion

We decomposed the database into two different groups: the former consists of 25 compounds as a training set and the latter consists of 5 compounds as a test set. The CoMFA model has an excellent value of non-cross-validated ($R^2 = 0.92$), Standard error of the estimate (Scv = 0.19), F of 59.72, with a cross-validated Q^2 (0.70), and an optimum number of components of three. Subsequently, these models showed that the electrostatic field has the highest contribution in this model with a value of 52%, while the steric field was found to be 48% and the external validation indicated a rext2 value of 0.96. The result of the CoMSIA model showed good values of $R^2 = 0.86$, cross-validated $Q^2 = 0.62$, coefficient value of external validation $rext^2 = 0.98$, an optimum component of 3, test value F=32.94, and standard error of the estimate Scv=0.24. The contributions of an electrostatic, steric, hydrophobic, h-bond donor, and h-bond acceptor field were 26%, 6%, 11%, 19% and 39% respectively, which means that the h-bond acceptor and electrostatic fields played important key roles in this model. The statistical results for the models CoMFA and CoMSIA are shown in table 2, while table 3 shows the experimental pIC_{50} values of the best models.

Table 2 : The PLS statistical results of methods models.

| Model	Q^2	R^2	SCV	F	N	$rext^2$	FRACTION				
							Ster	Elec	Acc	Don	Hyd
CoMFA	0.70	0.92	0.19	59.72	3	0.96	0.48	0.52	-	-	-
CoMSIA	0.62	0.86	0.24	32.94	3	0.98	0.06	0.26	0.39	0.19	0.11

Table 3 : 1,3,5-triazine derivatives studied and their observed and predicted anticancer activities.

N	pIC50 (M)	Predicted		N	pIC50 (M)	Predicted	
		CoMFA	CoMSIA			CoMFA	CoMSIA
1	5.25	5.34	5.32	16	4.67	4.55	4.71
2	5.07	5.09	5.08	17	5.32	5.4	5.41
3	5.33	5.13	5.19	18	5.15	5.41	5.11
4	4.66	4.94	4.92	19*	5.94	5.60	5.57
5	5.63	5.66	5.81	20	4.82	5.31	4.98
6	5.07	5.04	5.06	21*	5.82	5.62	5.63
7	5.95	6.17	6.06	22	5.11	5.01	5.18
8*	4.29	4.46	4.19	23	6.70	6.72	6.74
9	4.88	4.94	4.84	24	4.74	4.92	4.52
10*	4.80	4.63	4.73	25	5.00	4.75	5.10
11	5.05	5.00	4.93	26	5.18	5.00	4.90
12	4.63	4.78	4.74	27	4.93	4.82	5.02
13	5.84	5.69	5.86	28	5.37	5.40	5.38
14	4.67	4.74	4.82	29	5.27	5.30	5.20
15	6.49	6.27	6.41	30*	5.41	5.55	5.45

### 3.1. Graphical interpretation of CoMFA and CoMSIA

The contours maps of CoMFA/CoMSIA were created to visualize the model field distribution where the modifications may occur in an increase of the activity. Figures 3 and figure 4 display the CoMFA and CoMSIA contour maps, respectively. In the present study, compound 23 was employed as a reference structure, and all the contours represented the default 20% and 80% level contributions for unfavored and favored regions.

3.2. CoMFA and CoMSIA contour maps.
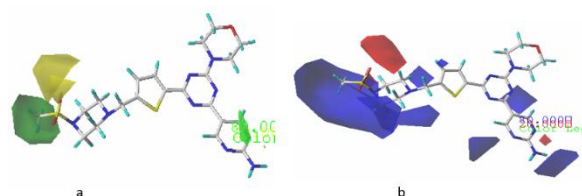
Figure . 3. CoMFA field. a: Steric, b: electrostatic

The steric contour maps (Fig, 3a). The green contours appeared around R2 positions, indicating that

bulky substitutions selection is necessary for this position (increase activity). This can explain the higher activity of compounds 7 (pIC$_{50}$ = 5.95) having 1-methanesulfonylpiperazine at the R$_2$ position, compared to the compound 4 (pIC$_{50}$ = 4.66) having piperidine group at this position. The yellow colors surround the oxygen atom at group R$_2$ position, indicating that adding a bulky substitute would be unfavorable to the activity potency. The electrostatic contour maps (Fig, 3b). The blue color is found close to R, R$_1$ and R$_2$ positions, indicating that substituents with electron-accepting character are unfavored at these positions (decrease activity). These findings might explain that the compounds 23 (pIC$_{50}$ = 6.70) with a pyrimidin-2-amine substituent at R1 position and 1-methanesulfonylpiperazine at R$_2$ position have a higher pIC50 value. In addition to that, a small red contour is near to the sulfonylmethane which belongs to the group R$_2$, which indicates regions where more negative charges are favorable for the activity.

_____
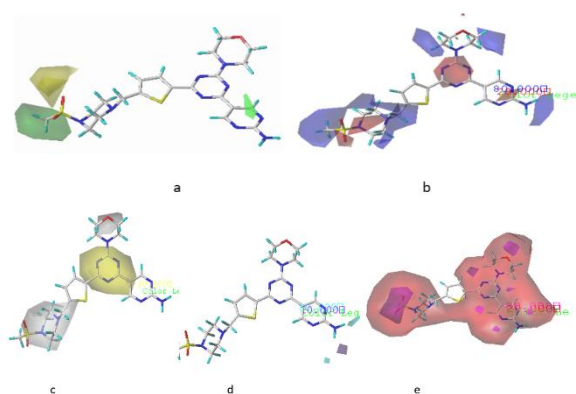
Figure . 4. CoMSIA field. a: Steric, b: electrostatic, c:
Hydrophobic, d: Hydrogen-bond donor, e: H-bond acceptor

The five fields of CoMSIA are presented in Fig 4 (a, b, c, d, and e). The steric and electrostatic effects are the same in the two models, so we are not talking about these fields. According to the results in table 2, the main fields that can describe the anticancer activity are electrostatic and h-bond accept due to their higher contribution of 26% and 39%, respectively.

The hydrophobic contour maps (Fig, 4c). Yellow and white colors mean that hydrophobic groups increase and decrease the anticancer activity, successively. The white contour is located near R_2 and the oxygen atom of morpholine, while yellow appears in 1,2,3 triazine.

The H-bond donor contour maps (Fig, 4d). Cyan and purple colors mean that the h-bond donor group improves and does not improve the activity of anticancer, successively. The cyan contour is located close to the two hydrogen atoms of R_1. The

contribution of this field is lower. This complicates use in the designs of new compounds.

The hydrogen bond acceptors contour maps (Fig, 4e). The red and magenta represent favorable and unfavorable positions for the hydrogen donor groups for increasing the anticancer activity. The magenta contour around the sulfonylmethane of the R_2 position indicates that a h-bond acceptor substituent at this position is favorable to increasing the activity, while the color red covers all compounds except the thiophene this explains the higher activity of compound 23 ($pIC_{50} = 6.70$) which has a hydrogen bond donor group (NH_2) at R_1, and this also explains the higher activity of compound 13 ($pIC_{50} = 5.84$) which has a donor group (OH) in R_1 compared to the activity of compound 4 ($pIC_{50} = 4.66$).

3.3. Y - randomization

To evaluate the sturdiness of the models, the pIC_{50} values were randomly shuffled, and after each rounding, a new QSAR model was obtained. The new values of Q^2 and R^2 are not acceptable because ($Q^2 < 0.5$, $R^2 < 0.6$), indicating that our optimal models are not due to a chance correlation. Q^2 and R^2 values of the generated models after several Y–randomization tests are shown in Table 4.
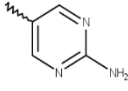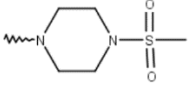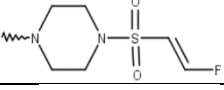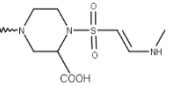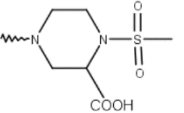
3.4. Newly designed compounds

According to the 3D QSAR modeling, we have designed four more active molecules with higher biological activity than the most active compound molecule 23 ($pIC_{50}= 6.699$). Table 5 displays the pIC_{50} values and structures of these molecules.

Table 4: Q^2 and R^2 values of the generated models after several Y – randomization tests.

Iteration	CoMFA		CoMSIA	
	Q^2	R^2	Q^2	R^2
1	-0. 328	-0.476	-0.358	-0.542
2	0.185	0.294	0.076	-0.081
3	0.090	0.132	0.163	0.295
4	-0.330	-0.261	-0.384	-0.289
5	0.312	0.415	0.213	0.424

_____

Table 5: The proposed structures of new molecules and their pIC50 values.

N°	R	R₁	R₂	CoMFA	CoMSIA
				Predicted pIC50	
23	H	(pyrimidine-NH₂ structure)	(piperazine sulfonyl methyl structure)	6 .70	6.73
X₁	Cl	–	(piperazine sulfonyl vinyl-F structure)	6.78	6.95
X₂	(allyl-F structure)	–	(piperazine sulfonyl NH structure, COOH)	6.86	6.89
X₃	F	–	(piperazine sulfonyl methyl structure, COOH)	6.78	6.86
X₄	Cl	–	–	6.90	6.96

3.5. ADMET prediction

Characterization of absorption, distribution, metabolism, and excretion (ADMET) is an essential step in predicting the properties of drugs. These features were obtained by using Swissadme and pKSM online tool successively. Table 6 shows the ADMET prediction of compound 23 and the proposed compounds (X₁-X₄).

Table 6: ADMET prediction of the most potent C23 inhibitor in the dataset and newly designed inhibitors.

Models		C23	X₁	X₂	X₃	X₄
Models		Compounds				
Absorption (A)						
Water solubility		-2.88	-2.35	-2.34	-2.06	-2.07
Intestinal absorption (human)		50.04	74.88	92.66	84.41	90.02
Distribution (D)						
Blood-brain barrier (logBB)		-2.03	-2.57	-2.39	-2.23	-2.20
Volume of distributionVDS		0.23	0.22	0.54	0.63	0.59
Metabolism (M)						
Substrate (CYP)	2D6	No	No	No	No	No
Substrate (CYP)	3A4	Yes	Yes	Yes	Yes	Yes
Inhibition (CYP)	1A2	No	No	No	Yes	No
Inhibition (CYP)	2C19	No	No	No	Yes	No
Inhibition (CYP)	2C9	No	No	Yes	Yes	No
Inhibition (CYP)	2D6	No	No	Yes	No	Yes
Inhibition (CYP)	3A4	Yes	Yes	Yes	Yes	Yes
Excretion (E)						
Clearence		0.61	0.87	0.83	0.72	0.81
Toxicity (T)						
AMES toxicity		No	No	No	No	No

The poor absorption is linked to the poor solubility of the drugs in water. Our objective is to eliminate the compounds which are soluble a little in water, i.e., which have water solubility values <-4. In this table, all compounds respect this value. Absorption corresponds to all the phenomena involved in the transfer of the active medicinal ingredient from its site

of administration to the bloodstream. In our table, we observe that all proposed compounds have a value greater than 70%. Therefore, they are better for the human intestines.

The volume of distribution or the apparent volume of distribution (V_{DS}) is a parameter characterizing the distribution of the active substance (in a drug) in the human body, and the brain is protected against hormones, toxins, pathogens circulating in the blood by the blood-brain barrier (BBB). The values are accepted if values (VDss) > 0.45 and (log BB <-1), respectively, the results obtained show that all compounds have (log BB <-1), but only the proposed compound X1 has (VDss) < 0.45.

Metabolism is the set of chemical reactions that take place inside a living being and allow it to stay alive, reproduce, develop, and respond to stimuli from its environment. In drug metabolism, studies show that so far there are 17 CYP families, but the CYP 3A4 plays a significant role. All compounds (X_{1-4}) are inhibitors and substrates of CYP3A4. At the level of excretion and toxicity, all compounds have good total clearance values, and are non-toxic. Based on these findings, only the compounds X_2, X_3, and X_4 were selected for the following analysis.

3.6. Docking results

To examine and see the 2D View binding modes of the proposed (X_2, X_3, and X_4) and 23 compounds with the active site of PI3Kα (PDB code: 4L233), we used molecular docking, in which the results obtained are shown in table 7.

All compounds have conventional hydrogen bond interactions, which increases the stability of these complexes. Moreover, only compound X_3 has unfavorable donor-donor interaction, the stability of this complex is decreased. To continue the comparison of the stability of these complexes. Table 8 shows the types of interactions and total scoring.

Table 7: 2D View of the binding conformation of the proposed and 23 compounds with the active site of PI3Ka.
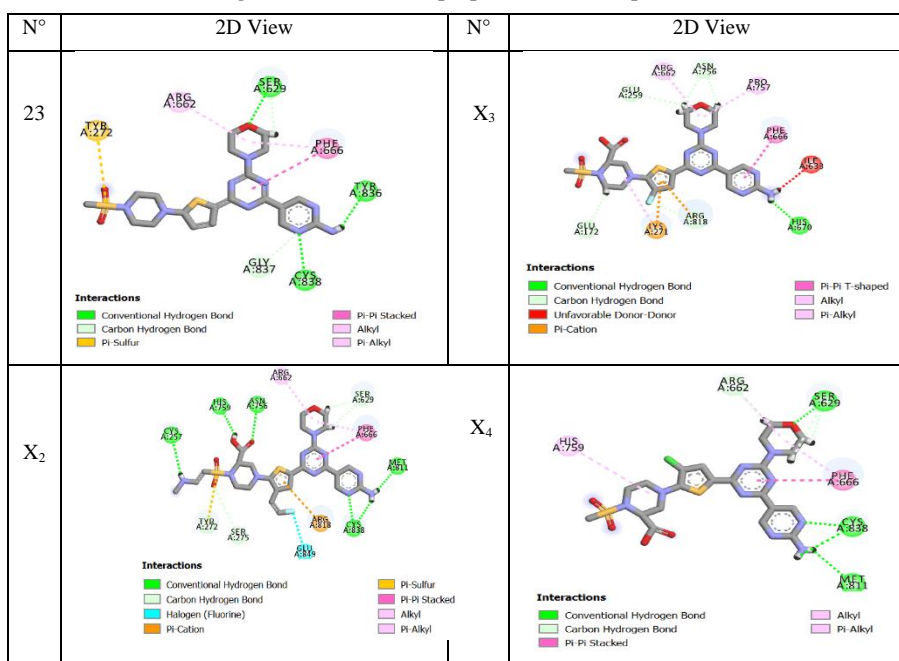
Table 8: Types of interaction and total scoring

N°	Types of interactions		Total scoring
	Hydrogen Bond	Unfavorable Donor-Donor	
23	Tyr A:836, Cys A:838, Ser A: 629	_	3.73
X_2	Cys A: 838, Met A:811, Asn A: 756, His A:759, Cys A:257.	_	6.03
X_3	His A:670.	Ile A:633	2.25
X_4	Met A: 811, Cys A:838, Ser A: 629 .	_	5.29

_____

Egypt. J. Chem. **65,** No. SI:13B (2022)

The most stable compounds are X_2 and X_4 due to the high values of total scoring (6.03 and 5.29), and in types of interactions H-bond, these compounds have not any unfavorable donor-donor, which we can conclude that the designed compounds (X_4 and X_2) are the most of bioactivity against cancer cell lines (human lung adenocarcinoma cells A549).

4. CONCLUSION

In this study, a series of thirty 1,3,5-triazine derivatives reported as PI3Kα inhibitors against cancer cell lines (human lung adenocarcinoma cells A549) A549, were studied using 3D-QSAR through CoMFA and CoMSIA models, showing efficient predictability and stability. The 3D-QSAR contour maps analysis helped to better interpret the feature requirements, revealing the key roles played by the electrostatic and hydrogen bonding substitutions to increase the bioactivity. Consequently, based on the useful guidelines developed by the 3D-QSAR study, four novel 1,3,5-triazine derivatives were proposed with high PI3Kα inhibitory activity. Furthermore, in silico ADMET study showed good properties for the new proposed PI3Kα inhibitors, except the X1 compound. The selected compounds were further analyzed using molecular docking, among which the compounds X2 and X4 bind closely to the active site of the receptor and showed favorable interaction. Furthermore, in silico ADMET study showed good properties for the new proposed anticancer inhibitors.

5. Conflicts of interest
"There are no conflicts to declare".

6. Acknowledgments
Great thanks to the "Association Marocaine des Chimistes Théoriciens" (AMCT) for its relevant help concerning the programs. All authors have given us their written permission to be named.

7. REFERENCES

1. Zhu W, Chen C, Sun C, Xu S, Wu C, Lei F, et al. Design, synthesis and docking studies of novel thienopyrimidine derivatives bearing chromone moiety as mTOR/PI3Kα inhibitors. European Journal of Medicinal Chemistry. 2015 Mar;93:64–73.
2. Xu S, Sun C, Chen C, Zheng P, Zhou Y, Zhou H, et al. Synthesis and Biological Evaluation of Novel 8-Morpholinoimidazo[1,2-a]pyrazine Derivatives Bearing Phenylpyridine/Phenylpyrimidine-Carboxamides. Molecules. 2017 Feb 17;22(2):310.
3. Sun C, Chen C, Xu S, Wang J, Zhu Y, Kong D, et al. Synthesis and anticancer activity of novel 4-morpholino-7,8-dihydro-5H-thiopyrano[4,3-d]pyrimidine derivatives bearing chromone moiety. Bioorganic & Medicinal Chemistry. 2016 Aug;24(16):3862–9.
4. Hennessy BT, Smith DL, Ram PT, Lu Y, Mills GB. Exploiting the PI3K/AKT Pathway for Cancer Drug Discovery. Nat Rev Drug Discov. 2005 Dec;4(12):988–1004.
5. Wang Q, Li X, Sun C, Zhang B, Zheng P, Zhu W, et al. Synthesis and Structure–Activity Relationships of 4-Morpholino-7,8-Dihydro-5H-Thiopyrano[4,3-d]pyrimidine Derivatives Bearing Pyrazoline Scaffold. Molecules. 2017 Oct 31;22(11):1870.
6. Burke RT, Meadows S, Loriaux MM, Currie KS, Mitchell SA, Maciejewski P, et al. A potential therapeutic strategy for chronic lymphocytic leukemia by combining Idelalisib and GS-9973, a novel spleen tyrosine kinase (Syk) inhibitor. Oncotarget. 2014 Feb 28;5(4):908–15.
7. Patnaik A, Appleman LJ, Tolcher AW, Papadopoulos KP, Beeram M, Rasco DW, et al. First-in-human phase I study of copanlisib (BAY 80-6946), an intravenous pan-class I phosphatidylinositol 3-kinase inhibitor, in patients with advanced solid tumors and non-Hodgkin's lymphomas. Annals of Oncology. 2016 Oct;27(10):1928–40.
8. Mayer IA, Abramson VG, Formisano L, Balko JM, Estrada MV, Sanders ME, et al. A Phase Ib Study of Alpelisib (BYL719), a PI3Kα-Specific Inhibitor, with Letrozole in ER + /HER2 − Metastatic Breast Cancer. Clin Cancer Res. 2017 Jan 1;23(1):26–34.
9. Knight SD, Adams ND, Burgess JL, Chaudhari AM, Darcy MG, Donatelli CA, et al. Discovery of GSK2126458, a Highly Potent Inhibitor of PI3K and the Mammalian Target of Rapamycin. ACS Med Chem Lett. 2010 Apr 8;1(1):39–43.
10. Wallin JJ, Edgar KA, Guan J, Berry M, Prior WW, Lee L, et al. GDC-0980 Is a Novel Class I PI3K/mTOR Kinase Inhibitor with Robust Activity in Cancer Models Driven by the PI3K Pathway. Mol Cancer Ther. 2011 Dec;10(12):2426–36.

_____

11. Park S, Chapuis N, Bardet V, Tamburini J, Gallay N, Willems L, et al. PI-103, a dual inhibitor of Class IA phosphatidylinositide 3-kinase and mTOR, has antileukemic activity in AML. Leukemia. 2008 Sep;22(9):1698–706.

12. Giard DJ, Aaronson SA, Todaro GJ, Arnstein P, Kersey JH, Dosik H, et al. In Vitro Cultivation of Human Tumors: Establishment of Cell Lines Derived From a Series of Solid Tumors2. JNCI: Journal of the National Cancer Institute. 1973 Nov;51(5):1417–23.

13. Foster KA, Oster CG, Mayer MM, Avery ML, Audus KL. Characterization of the A549 Cell Line as a Type II Pulmonary Epithelial Cell Model for Drug Metabolism. Experimental Cell Research. 1998 Sep;243(2):359–66.

14. Vilquin P, Cohen P, Maudelonde T, Tredan O, Treilleux I, Bachelot T, et al. Nouvelles stratégies thérapeutiques dans le cancer du sein hormono-dépendant métastatique. Bulletin du Cancer. 2015 Apr;102(4):367–80.

15. Ghayad S, Cohen P. Inhibitors of the PI3K/Akt/mTOR Pathway: New Hope for Breast Cancer Patients. PRA. 2010 Jan 1;5(1):29–57.

16. Benjamin D, Colombi M, Moroni C, Hall MN. Rapamycin passes the torch: a new generation of mTOR inhibitors. Nat Rev Drug Discov. 2011 Nov;10(11):868–80.

17. Fu X, Osborne CK, Schiff R. Biology and therapeutic potential of PI3K signaling in ER+/HER2-negative breast cancer. The Breast. 2013 Aug;22:S12–8.

18. Zhang B, Zhang Q, Xiao Z, Sun X, Yang Z, Gu Q, et al. Design, synthesis and biological evaluation of substituted 2-(thiophen-2-yl)-1,3,5-triazine derivatives as potential dual PI3Kα/mTOR inhibitors. Bioorganic Chemistry. 2020 Jan;95:103525.

19. Clark M, Cramer RD, Van Opdenbosch N. Validation of the general purpose tripos 5.2 force field. J Comput Chem. 1989 Dec;10(8):982–1012.

20. Purcell WP, Singer JA. A brief review and table of semiempirical parameters used in the Hueckel molecular orbital method. J .Chem .Eng Data. 1967April; 12 (2): 235-246.

21. Sybyl-X [Internet]. omicX. available on: https://omictools.com/sybyl-x-tool.

22. EL-Mernissi R, Khatabi KE, Khaldan A, Ajana MA, Bouachrine M, Lakhlifi T. Discoveryof orthotolyloxyacetamides as inhibitors of NOTUM using 3D- QSAR and molecular docking studies. 2020;11.

23. Cramer RD, Patterson DE, Bunce JD. Comparative molecular field analysis (CoMFA). 1. Effect of shape on binding of steroids to carrier proteins. J Am Chem Soc. 1988;110(18):5959-67.

24. Klebe G, Abraham U, Mietzner T. Molecular Similarity Indices in a Comparative Analysis (CoMSIA) of Drug Molecules to Correlate and Predict Their Biological Activity. J Med Chem. 1994;37(24):4130-46.

25. Bush BL, Nachbar RB. Sample-distance partial least squares: PLS optimized for many variables, with application to CoMFA. J Comput Aided Mol Des. 1993 ;7(5):587-619.

26. El Khatabi K, Aanouz İ, El-MerniSsi R, Khaldan A, Ajana MA, Bouachrine M, et al. Designing of Novel Potential Inhibitors of a-amylase by 3D-QSAR Modeling and Molecular Docking Studies. Journal of the Turkish Chemical Society Section A: Chemistry. 2020 May 10;469–78.

27. El Khatabi K, Aanouz I, EL-Mernissi R, Khaldan A, Ajana MA, Bouachrine M, et al. Discovery of novel potential anti-Alzheimer hydrazones derivatives using 3D QSAR and molecular docking studies. 2020;11.

28. Biswal RA, Sharma A, Aishwariya A, Pazhamalai V. Molecular docking and admet studies of bioactive compounds of rhizopora mucornata against bacterial enzyme protein tyrosine phosphatase. International Journal of Pharmaceutical Sciences and Research. 11:8.

29. Discovery Studio Predictive Science Application | Dassault Systèmes BIOVIA [Internet]. available on: https://www.3dsbiovia.com/products/collaborative-science/biovia-discovery-studio/.

30. DeLano WL. Pymol: An open-source molecular graphics tool. CCP4 Newsl Protein Crystallogr. 2002;40(1):82–92.

_____